

The Electrical Conductivity of Lherzolite

AL DUBA

Lawrence Livermore National Laboratory, Livermore, California

STEVEN CONSTABLE

Scripps Institution of Oceanography, La Jolla, California

Electrical conductivity as a function of oxygen fugacity (f_{O_2}) between 10^{-5} Pa and 1 Pa, temperature between 700°C and 1200°C, and time over a period of 1700 hours are reported for a lherzolite nodule from Mount Porndon, Australia. Analysis of complex impedance collected at 100 Hz, 1 kHz, and 10 kHz indicates that there is significant frequency dispersion in this rock at temperatures below 900°C–1000°C. By choosing the resistance of an equivalent parallel RC network at the frequency having minimum phase, the effect of dispersion is largely avoided. Conductivity as a function of time, collected following changes in f_{O_2} at 1010 and 1200°C, has been analyzed to determine the diffusivity of defects relating f_{O_2} to the electrical conduction mechanism in olivine. The diffusivities so obtained are in remarkably good agreement with those determined from strain measurements during creep tests, which implies that magnesium vacancies are the rate-limiting step for conductivity reequilibration after f_{O_2} changes. A longer-term process is observed in this rock in which the conductivity drifts upward or downward with a time constant of hundreds of hours after initial reequilibration to gas mix (f_{O_2}) changes. We speculate that this long-term drift could be related to equilibration of the iron distribution between coexisting olivine and pyroxene as a function of f_{O_2} . The sense is an increase in conductivity (olivine gains iron) at low f_{O_2} and vice versa. The lherzolite conductivity data are not significantly different from measurements made on olivine single crystals and polycrystals, even though the rock contains about 34 modal % pyroxene. This consistency of laboratory measurements of electrical conductivity of olivines from many localities and geological settings supports the use of recent models relating mantle temperature with electrical conductivity in the interpretation of mantle geo/electromagnetic soundings.

INTRODUCTION

Among geophysical methods, electrical conductivity σ affords a unique view of Earth's interior. This perspective comes from the high sensitivity of σ to temperature or to traces of materials at grain boundaries. Examples of such materials are fluids (aqueous or partial melt), ore minerals (sulfides and oxides), and elemental carbon (amorphous or graphitic). For instance, regions of recent volcanic activity and hydrothermal zones in the western United States are surface evidence for deeper movement of the lithosphere and upper mantle and for associated magma generation and transfer. In addition, such heat transfer processes and associated near-surface activities can lead to the development of hydrocarbons by supplying heat needed for maturation processes to occur during diagenesis of hydrocarbon-bearing sediments. Electrical methods are a means of probing such regions; their utility is increased if there are laboratory measurements to tie σ to geological conditions. Thus, the pyrolysis of oil shale, which can occur during diagenesis, leads to a large increase in electrical σ because of increased carbon at grain boundaries as light hydrocarbons are driven off [Duba, 1983]. Of more academic interest is the possibility of using the electrical conductivity of rocks that make up the mantle of Earth in conjunction with profiles of σ as a function of depth to determine the geotherm. The inverse approach was used by Cox *et al.* [1986] and Heinson and Constable [1992], who combined laboratory conductivity measurements with oceanic geotherms to estimate mantle

conductivity. In the case of Cox *et al.*, this constraint on atmospheric conductivity allowed a better determination of lithospheric mantle conductivity using field sounding data.

Electrical conduction in rocks has different aspects that can be treated separately. To begin with, nearly all the volumetrically abundant minerals by themselves are relatively insulating at sub-solidus temperatures. Earth's continental crystalline crust mainly consists of minerals such as feldspars or quartz that are very poor conductors having σ less than 10^{-5} siemens/meter (S/m) at temperatures below about 500°C [Oelhoeft, 1981; Kariya and Shankland, 1983]. Near the surface, these low conductivities are increased by the ubiquitous presence of water, which in extreme cases of high salinity can increase the conductivity of porous near-surface sedimentary rocks to 1 S/m or so. The middle and lower crust of even old, cold shields can also be relatively well conducting, having $\sigma > 10^{-2}$ S/m, and so it has been common in interpretations of crustal electromagnetic soundings to invoke the presence of highly conducting, interconnected grain-boundary phases such as water, melt, carbon, or sulphides or even the solid-state properties of grain boundaries between dissimilar minerals.

At uncontrolled oxygen fugacity, ultramafic rocks can have relatively high σ [Rai and Manghnani, 1978; Parkhomenko, 1967] when compared to that of single crystal pyroxene [Duba, Boland, and Ringwood, 1973; Huebner, Duba, and Wiggins, 1979] or olivine [Schock, Duba and Shankland, 1989] measured under controlled oxygen fugacity. Constable and Duba [1990] showed that ultramafic rocks having little or no alteration, exemplified by a dunite, have σ on the same order as that of single crystals when oxygen fugacity is controlled during conductivity measurements. The current report deals with electrical conductivity measurements made on lherzolite from Mount Porndon, Australia, which contains olivine, pyroxenes,

Copyright 1993 by the American Geophysical Union.

Paper number 93JB00995.
0148-0227/93/93JB-00995\$05.00

and secondary minerals. While a previous study by *Roberts and Tyburczy* [1991] examined a dunite containing 3% pyroxene, this study represents the first examination of material representative of upper mantle lherzolites in the 40–100 km depth range [*Irving*, 1980]. The presence of pyroxenes and secondary phases should act as a buffer for FeO, MgO, and silica. Such buffering is necessary if one is to obtain measurements on rocks that are representative of the situation extant in the mantle and to provide a well-defined thermodynamic state for the sample.

Olivine has been shown to control the conductivity of rocks in which it is the dominant mineral, and is assumed to control the conductivity of the upper mantle, where it is also the dominant mineral. The major defect responsible for electrical conduction in olivine at temperatures of 700–1300°C is inferred to be the “small polaron” Fe^{3+} ($= \text{Fe}_{\text{Mg}}^{\bullet}$ in Kröger-Vink notation) produced by oxidation of Fe^{2+} ($= \text{Fe}_{\text{Mg}}^{\times}$). Support for the polaron mechanism is provided by the positive thermoelectric coefficient below 1390°C [*Schock et al.*, 1989], dielectric measurements [*Sato*, 1986], and the increase of σ with iron content [*Hinze et al.*, 1982; *Hirsch, Shankland and Duba*, 1989; *Constable and Duba*, 1990]. Support is also provided by the positive dependence of σ on oxygen fugacity [*Schock et al.*, 1989].

EXPERIMENTAL TECHNIQUES

The lherzolite from Mount Porndon has approximate modal composition of 31% orthopyroxene, 3% clinopyroxene, 65% olivine (Fo 91.3), and 1% spinel (M. Drury, personal communication, 1992). The Fe/Mg content of the olivine is similar to that normally associated with mantle rocks, and petrological studies indicate a depth of origin of about 40–80 km for these xenoliths [*Irving*, 1980]. The grain size varies between about 0.5 and 1.5 mm. Although this rock is quite friable, we were able to core and cut it using a modification of a technique suggested by G. Bussod (personal communication, 1992). He had used naphthalene to hold the samples intact for coring and cutting operations. We found that using low-melting-point Crystal Bond[®] as the cement and removing it by dissolving in acetone was more convenient for polishing the electrode surfaces. The sample was cylindrical with a diameter of 7 mm and thickness of 1.15 mm. Electrical conductivity measurements were made in the apparatus described by *Duba et al.* [1990] at frequencies of 100 Hz, 1 kHz and 10 kHz. Electrical contact with the platinum electrodes welded to the Pt/Pt-10%Rh thermocouples was made via a 0.051 mm iridium foil on either side of the sample in order to minimize iron loss from the sample to the electrodes.

Oxygen fugacity (f_{O_2}) was controlled by passing a mixture of CO_2 and CO through the apparatus at atmospheric pressure. A total of 13,622 data were collected, consisting of triplets of time, conductivity, and temperature. Less frequently, measurements of gas mix f_{O_2} were made using a calcia-doped zirconia cell housed in a second furnace in series with the gas flow and held at 1200°C. These measurements were interpolated to add a fourth component to each conductivity datum. The entire $\sigma(\text{time})$ data set is shown in Figure 1. Large changes in $\sigma(\text{time})$ reflect changes in temperature, while the smaller steps in $\sigma(\text{time})$ are a result of changes in experimental f_{O_2} . Table 1 provides the pertinent parameters associated with all the runs which make up the experiment. Throughout this paper, values of f_{O_2} are quoted as measured at 1200°C; actual f_{O_2} at other temperatures is a function of the slope of the con-

stant gas mix curves [e.g., *Constable and Duba*, 1990], that is $-2.937 \log_{10}(\text{Pa})$ per $10^4/\text{K}$.

Evidence from *Wanamaker and Duba* [1993] suggests that significant iron loss does not occur at oxygen fugacities of 10^{-5} Pa or greater (at 1200°C), and so an f_{O_2} more reducing than 10^{-4} Pa was avoided in this experiment to prevent iron loss from the sample to the electrodes. Since iron loss from olivine reduces σ , repeat measurements of σ at fixed temperature and f_{O_2} throughout the experiment provides a good indication of how effective this procedure is. Although iron loss to the electrodes reduces σ , over the course of this long experiment the σ of the sample actually increased slightly, rather than decreased.

The sample was initially heated to 540°C at a rate of 2 K/min and at a gas mixture of $1\text{CO}_2/1\text{CO}$ in order to minimize oxidation caused by the CO/CO_2 gas mixture not being at equilibrium below this temperature, as pointed out by *Constable and Duba* [1990]. Above this temperature, heating and cooling rates were at 1 K/min and, on initial heating to 900°C, the gas mixture was changed to $30\text{CO}_2/1\text{CO}$. Extensive soaking of the sample at constant temperature at a set oxygen fugacity in the range 10^{-5} to 10^0 Pa (measured at 1200°C) allowed us to measure σ as a function of oxygen fugacity at 1010°C and 1200°C. The sample was allowed to equilibrate at least 5 hours for each gas mixture selected, and often for 50–100 hours. After the sample had equilibrated with a particular gas mixture, its σ was measured as temperature was decreased 400 K and as temperature was cycled back in preparation for the next gas mix change. In total, the sample spent over 1700 hours at temperatures above 540°C.

FREQUENCY DEPENDENCE OF CONDUCTIVITY

The conductivity apparatus collects complex impedance (Z) data at 100 Hz, 1 kHz and 10 kHz and computes derived parameters of resistance and capacitance assuming that these two circuit components are effectively in parallel for the sample. In the past we noted a lack of dependence of resistance on frequency for olivine rocks [*Constable and Duba*, 1990], and it has been practice only to report and interpret resistance measured at 1 kHz. Since resistance is a frequency-independent quantity as long as we remain within the grain-interior conduction regime [*Roberts and Tyburczy*, 1991], it will not exhibit dispersion even if impedance magnitude and phase does. However, some of the lherzolite data exhibits a much greater frequency dispersion than we have previously observed. In Figure 2 we plot σ computed from resistance versus $1/T$ for run AP, collected at an f_{O_2} of 10^{-3} Pa. Dispersion is evident below about 850°C and seems to be associated with a decrease in apparent activation energy.

Constable and Duba [1990] interpreted a similar but less pronounced decrease in activation energy below 700°C in dunite σ derived from 1 kHz resistance as a distinct, low-temperature, conduction mechanism. *Shankland et al.* [1991] suggested that this observation was a result of σ not being in equilibrium with the lower temperatures; that is, a higher-temperature, higher- σ state is partially frozen into the specimen on cooling. We will show below that the dispersion shown in Figure 2 is a result of errors in the computation of resistance at 1 and 10 kHz, and can be eliminated by using 100 Hz measurements at the lower temperatures. However, the issue of thermal equilibrium is important and arises later when we examine equilibration of σ with f_{O_2} , and so we investigate the effect of dis-equilibrium during temperature cycling and the

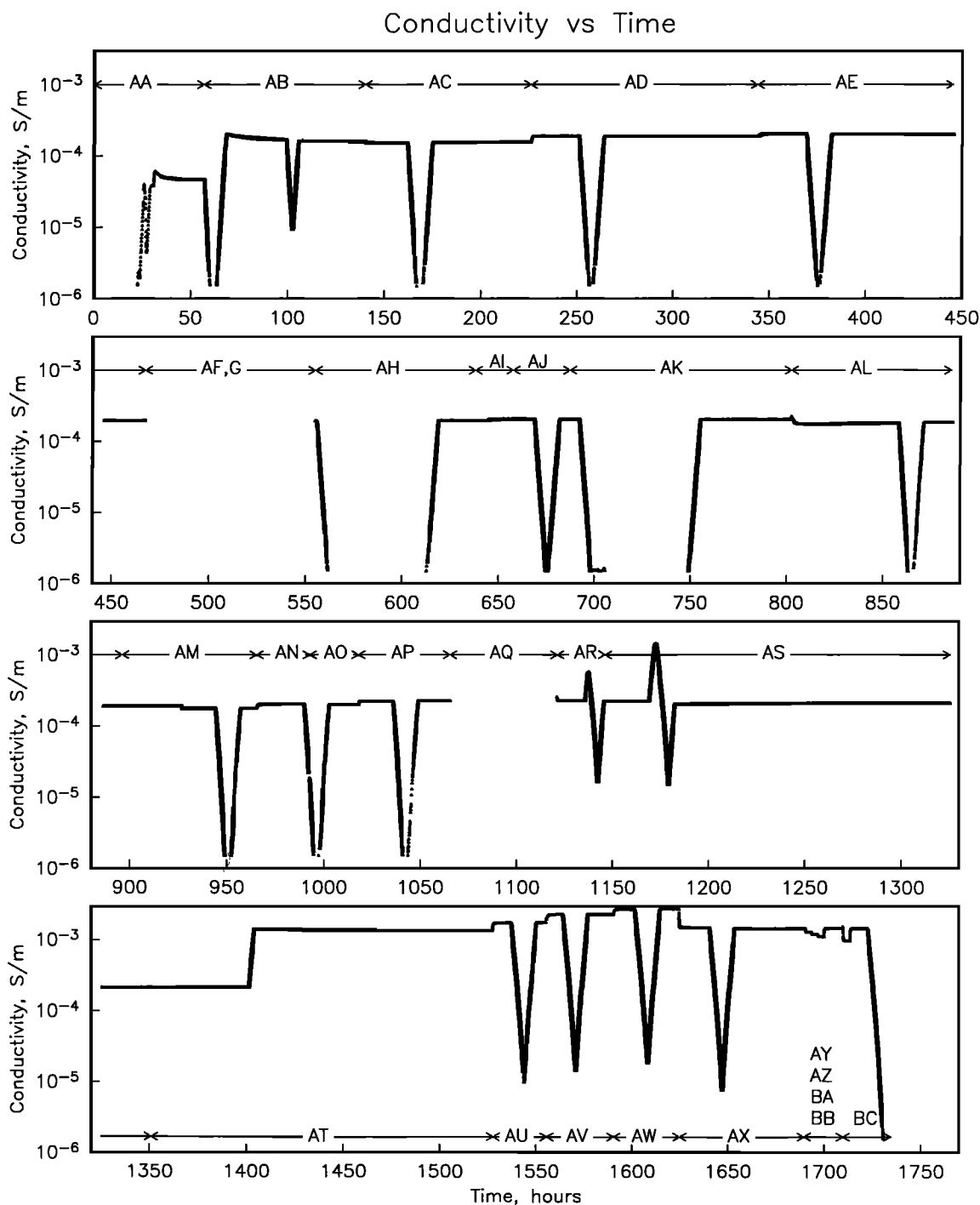


Fig. 1. Electrical conductivity versus time for the entire data set. Large variations in σ reflect changes in temperature, usually cycling to 600 or 800°C and back from higher temperature. Smaller variations in σ at around 2×10^{-4} (1010°C) or 10^{-3} S/m (1200°C) reflect changes in gas mix f_{O_2} . Data were lost for runs AF and AQ due to computer failure. The data plotted are the resistance of an equivalent parallel RC circuit, at either 100 Hz or 1 kHz, whichever has the smaller phase shift.

model of Shankland *et al.* [1991] quantitatively in the following section.

Although Shankland *et al.* discussed a more complicated situation which we consider below, we first evaluate simple exponential equilibrium, in which a change in temperature produces a change in σ as a function of time is given by

$$\sigma(t) = \sigma_o + (\sigma_e - \sigma_o)(1 - e^{-t/\tau}) \tag{1}$$

where σ_o and σ_e are the initial and equilibrium conductivities, and τ is the exponential time constant of the equilibration process. Equilibrium conductivity is given by the Arrhenius relationship

$$\sigma_e = \sigma_1 e^{-A/kT}. \tag{2}$$

This simple exponential model would be applicable, for example, to a lack of equilibrium with f_{O_2} conditions, discussed

TABLE 1. Experimental Parameters for Each Run Making Up the Experiment

Run	Time	T_{eq}	T_{min}	T_{max}	f_{O_2}	Comment
AA	16.93	900	20	900	-5, -3	heating from 20°C and equilibrate
AB	56.66	1010	600	1010	-3	cooling from 900 then reheating to 1010
AC	139.94	1010	600	-	-4	
AD	225.65	1010	600	-	-2	
AE	343.70	1010	600	-	-1	
AF	467.28	1010	600	-	-1	lower cooling rate, data lost
AG	-	-	-	-	-	run designation not used
AH	554.85	1010	600	-	-1	equilibrate at 600°C for 50h
AI	637.81	1010	-	-	-2	f_{O_2} change only
AJ	657.33	1010	600	-	-2	
AK	686.97	1010	600	-	0	equilibrate at 600°C for 50h
AL	802.27	1010	600	-	-4	
AM	895.97	1010	600	-	-5.5	f_{O_2} changed at 930h
AN/AO	965.23	1010	600	-	-4	
AP	1017.89	1010	600	-	-3	
AQ	1065.33	1010	600	-	-2	data lost
AR	1121.05	1010	800	1100	-3	first heating above 1010°C
AS	1145.94	1010	800	1200	-3	first heating above 1100°C
AT	1350.80	1010	-	1200	-3	heating to 1200°C and equilibrate
AU	1527.57	1200	800	-	-2	
AV	1555.48	1200	800	-	-1	
AW	1590.34	1200	800	-	0	
AX	1624.72	1200	800	-	-3	
AY	1689.46	1200	-	-	-3.5	gas change only
AZ	1693.88	1200	-	-	-4	gas change only
BA	1696.95	1200	-	-	-4.5	gas change only
BB	1700.14	1200	-	-	-3	gas change only
BC	1709.64	1200	20	-	-5, -3	f_{O_2} to -5, then -3, then to 20°C

T_{eq} , T_{min} , and T_{max} are the equilibration, minimum and maximum temperatures attained in each run, in degrees Celsius. f_{O_2} is quoted as the base 10 logarithm of f_{O_2} in pascals measured at 1200°C, and time is hours from the beginning of the experiment. Unless noted otherwise, gas changes are made at the beginning of a run.

by Constable and Duba [1990] for a case where the time constant is independent of environmental parameters. However, over a wide temperature range the time constant τ , which governs the generation of defects in response to a step increase in temperature, is itself thermally activated:

$$\tau = \tau_0 e^{E/kT} \quad (3)$$

where, according to Shankland *et al.* [1991], $E = 1.7$ eV, possibly based on observations of Fe-Mg interdiffusion by Buening and Buseck [1973]. Later we identify magnesium vacancies as the rate-limiting step for re-equilibration after f_{O_2} changes. If this represents the rate-limiting step for re-equilibration after temperature changes, then according to Mackwell *et al.* [1988] the activation energy should be about 1.9 eV, although we show later that this may in fact be closer to 1.7 eV.

Shankland *et al.* [1991] considered only the case of cooling from a high-temperature equilibrium state. In order to simulate one of our cooling and heating runs, we considered 200 steps of 4 K in temperature from 1000°C to 600°C and back to 1000°C, with each step taking 4 min (i.e. a heating and cooling rate of 1 K/min, as in the actual experiments). The time constant τ and equilibrium conductivity σ_e were computed for each temperature using equation (3) and (2), and the conductivity at the end of each 4-min step was computed using equation (1). This conductivity was then used as the initial conductivity for the next step. Lherzolite $\sigma(T)$, measured at high temperatures where equilibrium conditions are assumed to exist, gives $\sigma_1 = 485$ S/m and $A = 1.6$ eV and thus an equilibrium conductivity at 1000°C of $\sigma_e = 2.218 \times 10^{-4}$ S/m, which was used as the starting value for the simulation. The result of this simulated cooling and heating run is shown in

Figure 3a. By setting τ_0 equal to 10^{-5} min, a cooling run which reproduces the general appearance of the data can be obtained, but it is clear that the hysteresis observed in the subsequent heating run looks nothing like the real data in Figure 2. We can discard simple exponential disequilibrium as the cause for the apparent low-temperature conduction mechanism.

Shankland *et al.* [1991] actually proposed a more complicated dis-equilibrium model by considering that conductivity is given by

$$\sigma = qn\mu \quad (4)$$

where q is the charge of the defect species carrying current, n is the charge carrier density, and μ is the charge carrier mobility. They proposed that both n and μ equilibrate exponentially after changes in temperature, but with different time constants, so that

$$\sigma(t) = q[n_0 + (n_e - n_0)(1 - e^{-t/\tau_n})][\mu_0 + (\mu_e - \mu_0)(1 - e^{-t/\tau_\mu})]. \quad (5)$$

The time constants are both thermally activated, with $E = 1.7$ eV, but $\tau_n = 1000\tau_\mu$. The equilibrium conditions for n and μ are

$$n_e = n_1 e^{-A_n/kT} \quad (6)$$

and

$$\mu_e = \mu_1 e^{-A_\mu/kT}. \quad (7)$$

Shankland *et al.* [1991] set A_n at 1.4 eV and A_μ at 0.2 eV, giving a total activation energy of 1.6 eV. In order to finish defining the problem, we took an equilibrium number of carriers at 1000°C from Hirsch and Shankland [1993], $n_e = 10^{23} m^{-3}$, and from this obtained $n_1 = 3.53 \times 10^{28} m^{-3}$ using equation

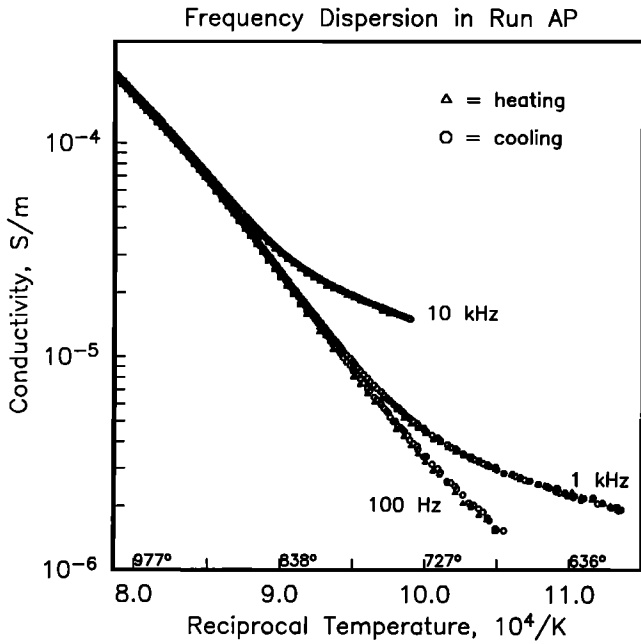


Fig. 2. Conductivity versus temperature measured at three frequencies for run AP. Conductivity is computed from real (Z), and all measurements are at an f_{O_2} of 10^{-3} Pa (measured at 1200°C). Both cooling and heating runs are shown, but hysteresis in temperature cycling is barely visible. However, frequency dispersion is evident below 850°C .

(6), then $\mu_{e(1000^\circ\text{C})} = 1.39 \times 10^{-8} \text{V}^{-1} \text{m}^2 \text{s}^{-1}$ using equation (4) and the equilibrium conductivity at 1000°C , and finally obtained $\mu_1 = 8.60 \times 10^{-8} \text{V}^{-1} \text{m}^2 \text{s}^{-1}$ using (7). Caution might be advised in abstracting any of these parameters for calculations from which more than a qualitative result is required, as the original intent of *Shankland et al.* [1991] was to demonstrate a qualitative fit to the data.

The results of the second simulation are shown in Figure 3b, and we see that while the change in slope of the cooling curve is more gentle and thus more realistic, the heating curve again displays severe hysteresis not seen in the real data. The more complicated model of thermal dis-equilibrium proposed by *Shankland et al.* [1991] does not fit the data either. The exact shape of these cooling/heating simulations can obviously be changed by varying the values of the various parameters in equations (5), (6) and (7), but the hysteresis between cooling and heating appears as a constant feature. Any combination of parameters that produces a shallowing of slope at low temperatures necessarily produces hysteresis. We note that the mathematics of any disequilibrium processes will be essentially the same as for temperature, so if there is, for example, a chemical disequilibrium that affects σ this will also be evident as hysteresis during cooling and heating. We conclude that the absence of hysteresis between cooling and heating indicates that, in spite of the cooler temperatures, the data shown in Figure 2 are in thermal equilibrium with respect to σ .

There are other tests that can be made to establish the existence of equilibrium at low temperatures. One is to change the heating and cooling rate to see if there is a change in apparent activation energy (slope in σ -reciprocal temperature). This was done in run AF, but unfortunately these data were lost as a result of a computer malfunction. However, in each of runs AH and AK we also held the sample at 600°C for 50 hours to examine long-term drift that might be associated with thermal disequilibrium, but saw none.

Roberts and Tyburczy [1991] are able to distinguish grain interior, grain boundary and electrode conduction in sintered olivine by examining Z over a frequency range of 10^4 to 10^{-4} Hz. Although we have only three frequencies spaced only two decades apart, we can plot phasor diagrams for comparison with their data. The results are shown in Figure 4, and direct comparison with Figure 5 of *Roberts and Tyburczy* shows great similarity of behaviour. That is, we see impedance

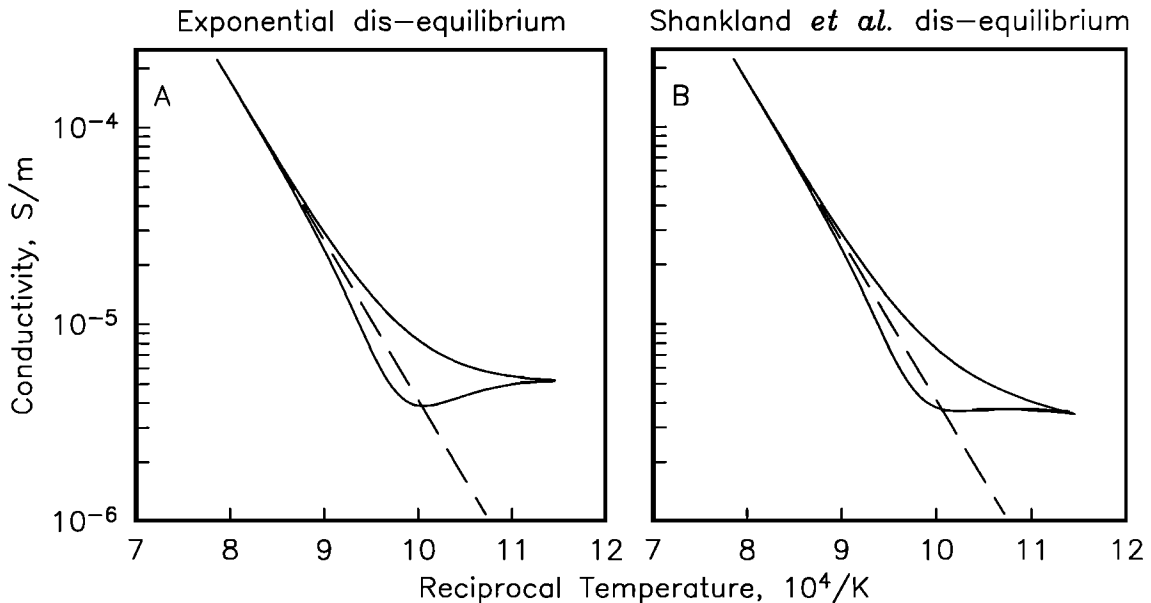


Fig. 3. (a) A simulation assuming simple exponential disequilibrium of the low-temperature conductivity measurements. The sample is assumed to have cooled from 1000°C to 600°C and then re-heated. The equilibrium conductivity is shown by the dashed line. It is clear that such disequilibrium will be manifest as large hysteresis during temperature cycling. (b) A similar simulation using the double time constant model of *Shankland et al.* [1991]. Although the cooling curve reproduces the features seen in the data of Figure 2, the heating curve again displays a great deal of hysteresis.

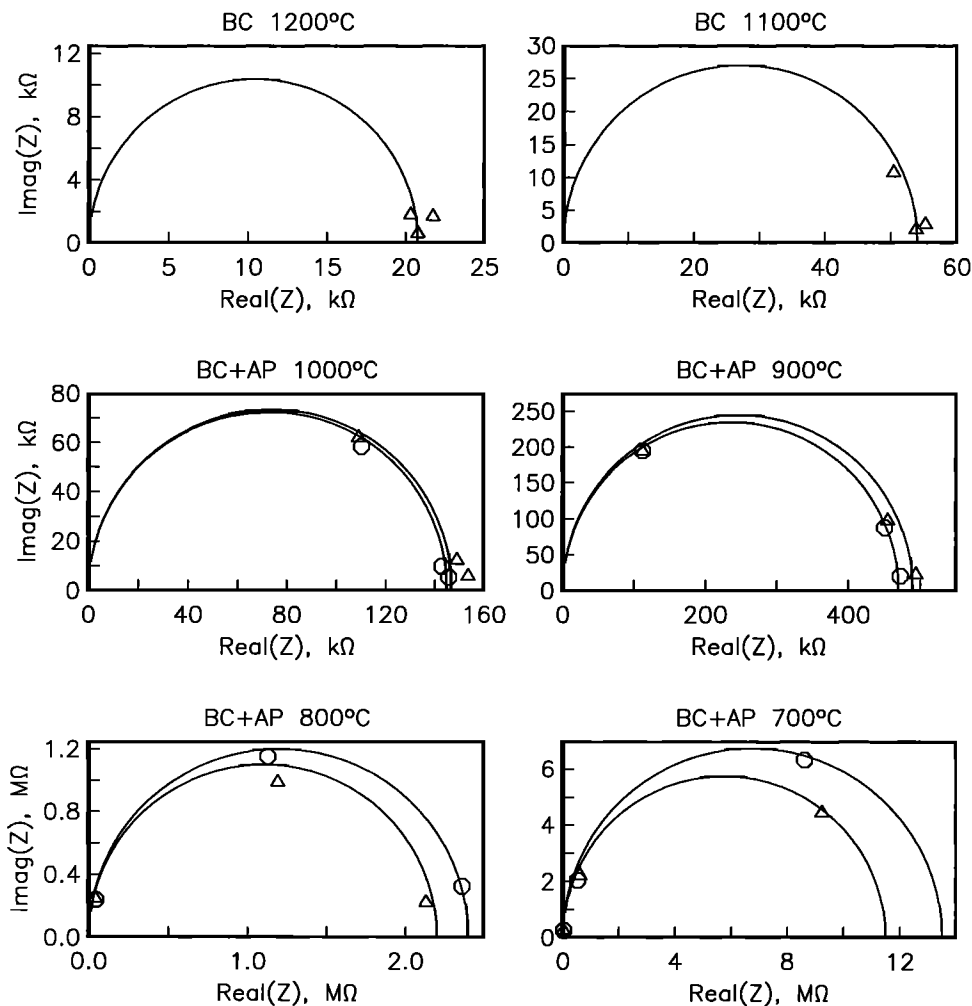


Fig. 4. Phasor diagrams, $\text{imag}(Z)$ versus $\text{real}(Z)$, of the complex impedance of data abstracted from runs AP and BC at the 6 temperatures indicated in the figures. The three frequencies are 100 Hz, 1 kHz and 10 kHz, always progressing from 10 kHz closest to the imaginary axis to 100 Hz furthest from the imaginary axis. While the data are sparse, the morphology of the dispersion is almost identical to that seen by *Roberts and Tyburczy* [1991]. The semicircular arcs centered on the real axis are for illustrative purposes, and do not represent a formal fit to the data.

dispersed along an arc centered on the real axis, extending (with decreasing frequency and increasing temperature) from the origin through the complex plane and back to the real axis at the value of the grain interior resistance. For 10 kHz, at 1100 and 1200°C we see the beginning of the next impedance arc, presumably associated with grain boundary conduction. It is true that we are limited by only having three frequencies available for this analysis, but we have essentially continuous temperature coverage and have the benefit of knowing the expected shape of the diagrams from the more extensive work of *Roberts and Tyburczy*.

The equipment at the Livermore facility computes resistance, during data acquisition, based on a simple parallel circuit of resistance and capacitance. That is, the equipment assumes that the data lie somewhere on a single arc centered on the real axis and intersecting the origin, just as drawn in Figure 4. In previous studies reporting data from the Livermore laboratory, conductivities exclusively derived from this resistance at 1 kHz have been published and interpreted. We note that based on both the lherzolite data and olivine data published by *Roberts and Tyburczy* [1991], above 900°C the 1 kHz resistance is always within a few percent of the diam-

eter of the grain interior impedance arc, and for the purposes of examining olivine σ behaviour, especially in single crystals, this component of the data is as good as any other. However, as temperature decreases the impedance migrates around the grain interior arc and it becomes increasingly difficult to estimate the diameter of the arc from the high-frequency data. Thus we see that the 10 kHz data migrate from the right-hand intercept at 1200°C to the left-hand intercept (the origin) at 700°C. Estimates of resistance (diameter of the arc) become increasingly inaccurate and evidently biased towards lower resistance and thus higher σ . This explains the dispersion seen in Figure 2; as the frequency increases so does error in the determination of σ . The algorithm used by the apparatus fails below 730°C for the 10 kHz data and computations of resistance are no longer available at this frequency. *Constable and Duba* [1990] reported conductivities down to 700°C based on 1 kHz resistances and interpreted them in terms of a low-temperature conduction mechanism. It is now clear that this is an erroneous interpretation resulting from error in resistance determination at 1 kHz at the lowest temperatures. This effect was dominant in only one early run using a particularly thin sample of dunite, and was not pronounced in later runs in which fre-

quency dispersion of resistance was examined [Constable and Duba, 1990, Figure 9] partly because a thicker sample and the lower σ of the dunite prevented measurements being made below 750°C and partly because the resistance computations faithfully recorded the diameter of the grain interior arc at all frequencies.

We note that although there is evidence of a grain interior arc in the 100 Hz data above 1000°C, the sample is much thinner than would be used if the primary concern was the characterization of grain boundary conduction. Thus many of the grains span the thickness of the sample without being interrupted by a grain boundary. The broadband measurements of Roberts and Tyburczy [1991] have proved essential for the interpretation of the lherzolite data, and clearly it would be desirable to extend the frequency range and density of measurements in a study such as this. However, we would like to point out that this does not necessarily mean that all measurements must be taken over the entire spectrum. These improvements in our understanding of olivine conductivity have made little impact on the interpretation of data above 1000°C because of the reliability of the 1 kHz resistance as a measure of grain-interior conductivity. Also, time spent making measurements at the lowest frequencies using the two-electrode method provides only an estimate of electrode impedance, which is usually of no interest as long as it does not contaminate the measurement of sample conductivity, and would prevent rapid measurements as a function of time, exploited below to recover diffusivities.

To avoid problems associated with the unreliability of the low-temperature/high-frequency resistances, and the possible migration into a grain-boundary conduction mechanism at high-temperature/low frequency, we have computed σ from the resistance at the frequency producing least phase shift, rather than simply resistance at 1 kHz. This provides a simple estimation of the diameter of the grain interior impedance arc and is used to derive the conductivities plotted in Figure 1. Processed in this way, the low-temperature conduction mechanism disappears (Figure 7) and we apparently have a single conduction mechanism down to 700°C and no discernible hysteresis on temperature cycling.

We see from Figure 4 that between runs AP and BC the grain interior resistance decreases at temperatures below 900°C up to a maximum of 15% at 700°C. This effect is small on a logarithmic scale (see Figure 7) and is equivalent to a slight decrease in apparent activation energy at low temperature over the time of the experiment. The absence of any change in σ above 900°C precludes a simple decrease in overall resistance of the sample, such as by sintering. Since the low-temperature measurements are within the grain interior arc, the effect is presumably not associated with improvement of electrode or grain boundary contact during the experiment. Since there is no evidence of a distinct low-temperature conduction mechanism, particularly in run BC, modification of such a conduction mechanism does not provide the explanation for increased σ with time. The lack of hysteresis with temperature cycling in run AP implies that we are not observing variations due to a lack of σ equilibrium. We are evidently altering the sample in some small, unknown, way, but the effect is negligible on the conclusions drawn in the rest of the paper.

CONDUCTIVITY VERSUS TIME

On initial heating from 540°C up to 900°C at a gas mixture of 30CO₂,1CO, σ increased dramatically at about 600°C and began to decrease at about 700°C (Figure 5). Following

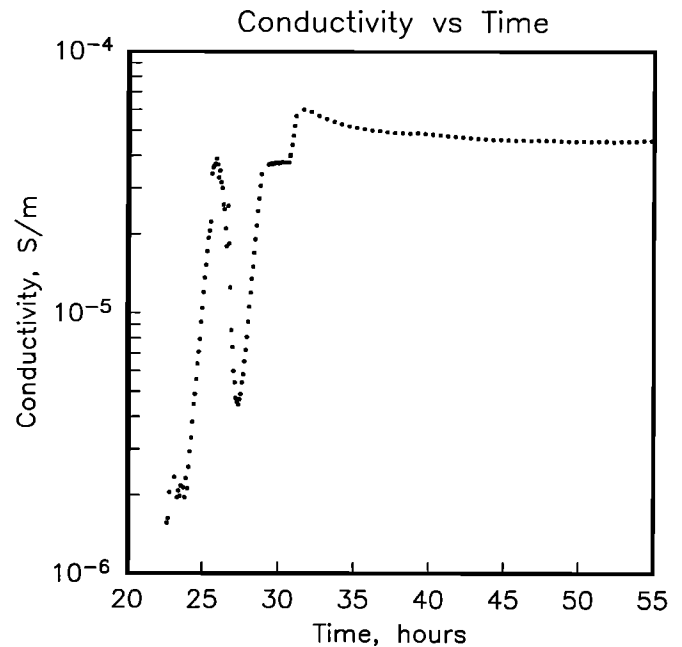


Fig. 5. Enlargement of σ -time plots for run AA and the first half of AB. The ragged peak in σ on initial heating (hours 23–27) is ascribed to carbon contamination from the gas mix and disappears around 670°C, where the gas mix leaves the edge of the carbon field. The flattening of σ between hours 29 and 30.5 is due to a halt in the heating at 878°C. Initial equilibration at 900°C (hour 31 onward) is toward lower conductivities and has a time constant of the order of 10,000 min.

Constable and Duba [1990], we ascribe this behavior to the disequilibrium precipitation of carbon from the gas mixture. Evidence that precipitation of carbon is the reason for this behavior is fairly strong: the appearance and disappearance of the carbon peak is consistent with the carbon field as defined by Deines *et al.* [1974] and samples removed after initial heating to only 700°C have visible carbon surface contamination. Above about 800°C the σ -temperature behavior of the sample is no longer affected by carbon and, after 25 hours at 900°C, σ had decreased 0.15 of a log unit. Conductivity measurements during subsequent temperature cycles down to 600°C showed no evidence of the presence of carbon. Following the 25 hour soak at 900°C, σ was measured with good reproducibility to 600°C on cooling and heating. The temperature was increased to 1010°C where the sample σ decreased about 0.1 of a log unit during 35 hours at that temperature. The time constant for this decrease, estimated in the manner described below, is on the order of 10,000 min. We interpret these slight decreases in σ to be the consequence of the removal of oxidation products caused during the sample's ascent to the surface and during cooling in the basalt flow with access to oxygen fugacity outside the stability of the rock's mineral assemblage as pointed out by Duba and Nicholls [1973]. Conductivity measured on cooling to 600°C and reheating to 1010°C showed excellent reproducibility and, after another 10 hours at 1010°C at the same gas mixture, σ decreased another 0.01 of a log unit with no further decrease noted in the ensuing 20 hours that the sample was maintained at this temperature and oxygen fugacity.

An interesting feature noted in the σ -time plots obtained for gas changes at 1010°C was a long-term drift in σ after initial equilibration to the gas change (Figure 6). The sense of this drift was a function of the oxygen fugacity: at 10⁻⁴ Pa,

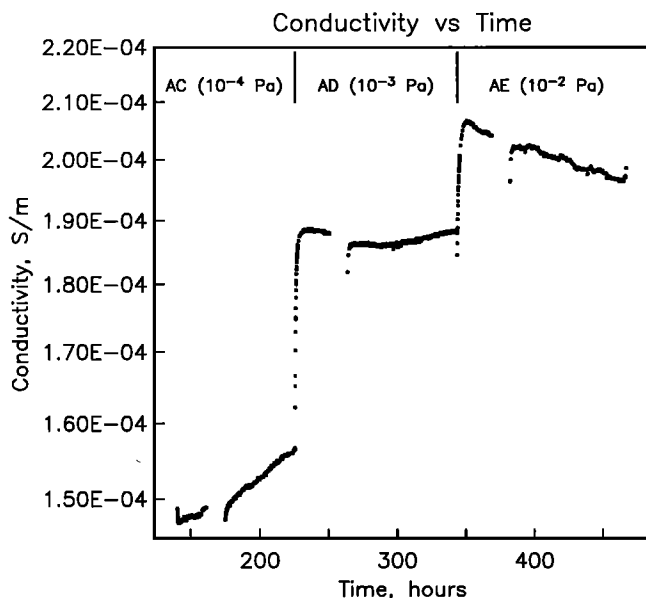


Fig. 6. Enlargement of σ -time for runs AC, AD, and AE, showing data collected mostly at 1010°C and at f_{O_2} of 10^{-4} , 10^{-3} , and 10^{-2} Pa, respectively. An exponential re-equilibration after each gas mix change occurs on a time scale of about 200 min and is discussed and modeled using theory presented in the paper, but after initial re-equilibration with the gas mix, σ drifts on a time scale of hundreds of hours. The small sinusoidal variation evident in AE is caused by a diurnal temperature-driven variation in gas flow, and hence f_{O_2} , because one of the gas flow meters is set near the limit of its operating range to attain the higher value of f_{O_2} .

the drift was toward increasing σ ; at 10^{-3} and 10^{-2} Pa, no drift was observed; and above 10^{-2} Pa, the drift was toward decreasing σ . The conductivity changes involved are small, but the effect is above the noise level of the measurements and systematic. Since this lherzolite contains pyroxenes in contact with olivine, we postulate that the drift is related to an oxygen-fugacity dependence of the K_d for iron in olivine-pyroxene pairs. The drift is consistent with iron gain by olivine from the pyroxene at low oxygen fugacity and loss from olivine to pyroxene at high oxygen fugacity. Since the sample appears to be equilibrated at 10^{-2} and 10^{-3} Pa, this suggests that the K_d for the rock was established at this condition. However, the 0.4 of a log unit decrease in σ noted in the initial heating at 10^{-3} Pa could also be due to a change in K_d since it is of the same order with respect to time constant. Thus, our initial heating could have set the K_d of this sample at 10^{-3} Pa. If this is the case, then the sample had last equilibrated its K_d at a higher oxygen fugacity than 10^{-3} Pa (1200°C) if the above model for the drift is correct. Experiments to check this hypothesis are planned since, if the model is correct, we have a means to determine the oxygen fugacity with which the sample was last in equilibration. Since the time required to re-equilibrate is at least 100 hours at 1010°C, this offers a possibility to determine the oxygen fugacity of the mantle source region of the lherzolite nodule before eruption, since it is unlikely that the nodule remained at temperatures in excess of 1000°C for more than a few hours after being explosively separated from the basalt flow which brought it to the oxygen-rich atmosphere of Earth's surface.

The rate of drift was higher for increases in σ associated with low f_{O_2} (10^{-4} Pa) than for decreases in σ associated with higher f_{O_2} . This tendency towards higher conductivities

was exacerbated by a slight hysteresis in f_{O_2} cycling. That is, decreasing f_{O_2} did not completely remove the σ enhancement resulting from previous increases in f_{O_2} . We do not currently understand either of these phenomena, but the combined effect produced an increase in σ from 1.6×10^{-4} S/m at the end of the initial re-equilibration (run AB) to 2.2×10^{-4} S/m just prior to heating to 1200°C (run AT), or 0.14 log units over 1400 hours, although most of this increase was accomplished prior to run AP (1000 hours). On the one hand this represents remarkable stability for this sort of experiment, but on the other hand the drift is comparable in magnitude to the systematic variations in σ we expect to interpret, such as dependence on f_{O_2} and Fe content. The hysteresis in f_{O_2} cycling is definitely evident in the 1200°C data, but we did not spend sufficient time at this temperature to examine the long-term drift. We particularly avoided low f_{O_2} in order to minimize iron loss to the electrodes, as suggested by *Wanamker and Duba* [1992], which is ironic because iron loss from olivine would reduce σ .

Figure 7 shows σ measured between 730 and 1200°C during runs AP, AT and BC at a gas mix which yields 10^{-3} Pa. Data are shown for the conductivity of the sample on cooling and heating between 1010 and 730°C as measured after equilibration at 1010°C, on heating to 1200°C from 1010°C for the first time, and on cooling to 730°C after more than 1200 hours at 1200°C. The remarkable consistency of σ at this gas mix throughout this part of the experiment confirms the reproducibility of the data and shows that no significant iron loss to the iridium has occurred. Activation energies for runs AX and BC are 1.616 and 1.614 eV respectively, in excellent agreement with the dunite results of *Constable and Duba* [1990] (1.60 eV), the sintered San Carlos olivine of *Tyburczy and Roberts* [1990] (1.49 eV) and [010] direction of single crystal San Carlos olivine reported by *Constable, et al.* [1992] (1.66 eV). The initial result for the lherzolite of 1.92 eV reported by *Constable et al.* [1992] was taken from run AB,

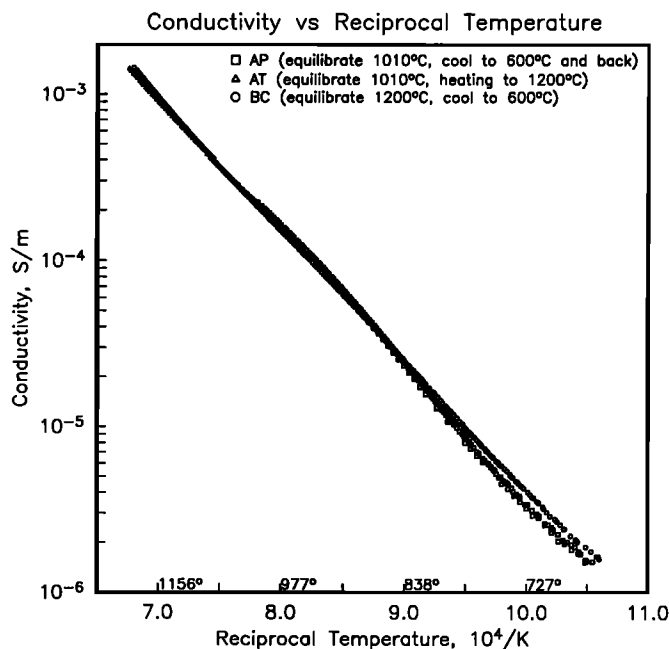


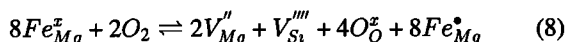
Fig. 7. Log conductivity versus reciprocal temperature for runs AP, AT and BC. All three runs were at an f_{O_2} of 10^{-3} Pa at 1200°C but spread over a time period of 29 days. The extremely good reproducibility of conductivity indicates that no significant iron loss to electrodes or other laboratory metamorphism is taking place.

before the sample had completed its initial equilibration, and is now seen not to be representative.

CONDUCTIVITY VERSUS f_{O_2}

Figure 8 shows that the variation of σ as a function of oxygen fugacity of this silica-activity-buffered (and perhaps iron-activity-buffered) olivine-rich rock is quite similar to that reported for buffered San Carlos olivine [Wanamaker and Duba, 1992] and dunite containing pyroxene and spinel from San Quintin, Mexico [Roberts and Tyburczy, 1993]. Dunite from Jackson County containing no pyroxene and little spinel [Constable and Duba, 1990], a similar rock designated North Carolina dunite [Roberts and Tyburczy, 1993], and single crystal Red Sea Peridot [Schock et al., 1989] exhibit a steeper slope at 10^{-5} to 10^{-3} Pa O_2 and lower conductivities at lowest f_{O_2} .

We have noted that the currently accepted model for $\sigma(T)$ in olivine is by means of polarons localized on Fe^{3+} . The relationship between conduction by such polarons and f_{O_2} is described by the reaction in which oxygen is adsorbed and forms the polarons:



[Schock et al., 1989]. This model predicts that σ will have a dependence on f_{O_2} of the form

$$\sigma = \sigma_0(f_{O_2})^{1/5.5} \quad (9)$$

This equation will hold for the other charge defects in equation (8), namely V_{Mg}'' and V_{Si}'''' . The data in Figure 8 have a slope much shallower than 1/5.5 and cannot be fit using such a model. Constable and Duba [1990] noted these small slopes and the tendency for the slope to decrease even further at low f_{O_2} , and suggested a model of threshold and f_{O_2} -dependent conduction:

$$\sigma = \sigma_0 + \sigma_1(f_{O_2})^c \quad (10)$$

Their least squares fitting with all of σ_0 , σ_1 , and c as free variables reproduced Jackson County dunite, Red Sea Peridot and San Carlos olivine data well. However, the least squares solution for the exponent c was about 1/3, which is inconsistent with the mechanism of equation (8). The slope was poorly constrained, however, as there were at that time no data for f_{O_2} greater than 10^{-2} Pa. If we re-do this fitting using the Marquardt method but this time constrain the exponent to be 1/5.5, we obtain the results shown in Figure 8 as solid lines and the parameters given in Table 2. This model fits the data acceptably well, but not as well as with the steeper slope. The difference is minor, however, and not enough to discard the model of equation (8), which is well supported by other measurements and theory.

Hirsch and Shankland [1993] proposed that at low f_{O_2} electrons would become the dominant charge carrier, and suggested a model with two f_{O_2} dependent defect populations:

$$\sigma = \sigma_0(f_{O_2})^{-1/5.6} + \sigma_1(f_{O_2})^{1/5.6} \quad (11)$$

The exponent of 1/5.6 presumably comes from the defect model used by these authors. We have maintained the more conventional 1/5.5 in our analysis. If we invert this equation, allowing σ_0 and σ_1 to be free parameters, we obtain the models shown as broken lines in Figure 8 and the parameters given in Table 2. This model fits the Red Sea Peridot data well, but is poorer for the other data sets, to the point of clear unacceptability in the case of buffered San Carlos olivine and San Quintin dunite. A second component to the simple model described by equation (9) is clearly required, but its f_{O_2} dependence is probably between zero and -1/5.6 and perhaps variable between samples. Wanamaker and Duba [1993] observed similar behaviour between unbuffered and pyroxene-buffered single crystal San Carlos olivine; the electron-polaron model of Hirsch and Shankland [1993] fit well to unbuffered

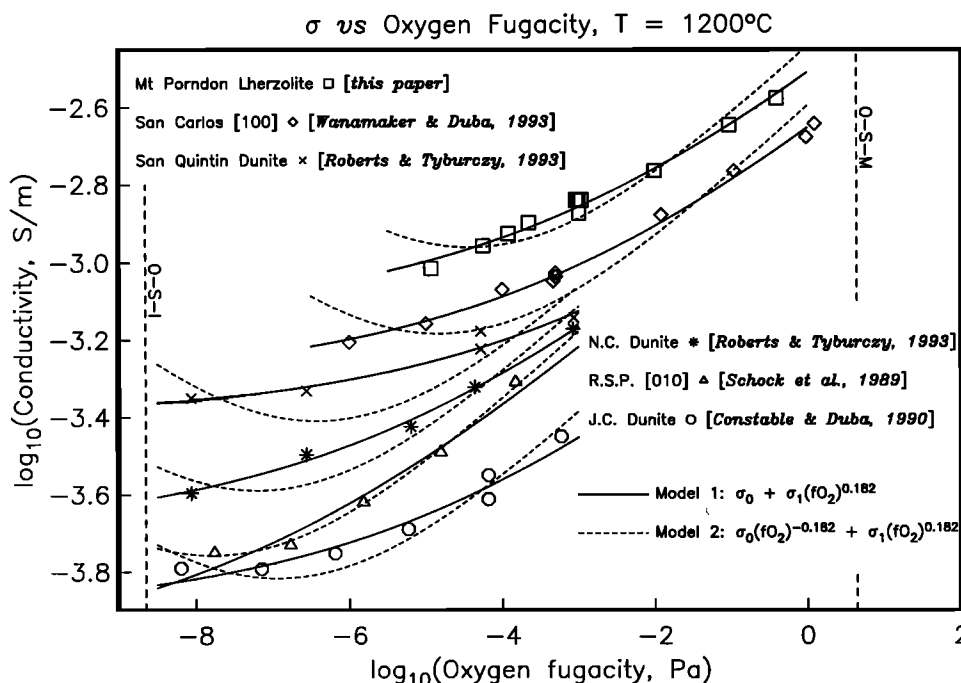


Fig. 8. Log conductivity versus log f_{O_2} at 1200°C for the lherzolite and other olivines. All the data are fit well by a threshold/ f_{O_2} -dependent model of defect production (solid line) with the exception of the single crystal Red Sea Peridot, which is fit slightly better by a model that includes electron conduction at low f_{O_2} (dashed line). None of the data fit an unmodified f_{O_2} -dependent model with a slope of 1/5.5.

TABLE 2. Parameters Fit to the Data Shown in Figure 8 Using Equations (10) (C-D Model), and (11) (H-S Model).

Rock Type	C-D Model			H-S Model		
	$\log_{10}\sigma_0$	$\log_{10}\sigma_1$	RMS	$\log_{10}\sigma_0$	$\log_{10}\sigma_1$	RMS
Mount Porndon lherzolite	-3.14	-2.63	3.1	-4.07	-2.46	9.4
San Carlos olivine [100]	-3.31	-2.76	3.1	-4.36	-2.61	14.0
San Quintin dunite	-3.40	-2.91	4.4	-4.88	-2.54	13.7
North Carolina dunite	-3.70	-2.77	2.5	-5.20	-2.58	10.1
Red Sea Peridot	-4.03	-2.75	6.2	-5.48	-2.64	2.1
Jackson County dunite	-3.91	-3.09	5.9	-5.38	-2.86	7.1

RMS is root-mean-square misfit of the model to conductivity data, in percent.

data, but the parametric model of *Constable and Duba* [1990] fit the pyroxene-buffered data better, although small negative powers of f_{O_2} were not incompatible with the data, either. The conclusion is that the effect of silica or iron buffering has a pronounced effect on the low- f_{O_2} σ behaviour of olivine.

Constable and Duba [1990] make the argument that the shallowing of $\sigma(f_{O_2})$ at low f_{O_2} is not the result of mixed conduction of two different defects because an Arrhenius plot of the data at 1200°C shows a nearly perfect line (Figure 7), implying only one activation energy. Mixed conduction does not appear for another 200 K, where magnesium vacancies are thought to dominate; the Seebeck coefficient reverses sign in San Carlos olivine at about 1390°C [*Schock et al.*, 1989], and *Constable and Duba* [1990] compute that there is an equal contribution to conductivity from polarons and magnesium vacancies at 1500°C in San Carlos olivine and Red Sea Peridot. Activation energies derived from runs AU to BC, which span f_{O_2} from 10^{-3} to 1 Pa, are essentially the same and all within 0.04 eV of 1.58 eV. Indeed, the highest and lowest activation energies, from runs AS and AX, are at the same f_{O_2} . It is possible that conduction between 600 and 1500°C is a result of mixed conduction by two species of defects which have such similar thermal activation energies that the experiment could not distinguish between them. It is an article of faith that Nature would not be so unkind as to arrange things this way. Although we cannot rule out a sudden change in activation energy below our limit of observation at 10^{-3} Pa, the *Hirsch and Shankland* [1993] model of mixed polaron and electron conduction implies that two significantly different activation energies would be evident as a function of f_{O_2} and temperature. To the extent that equation (10) represents a correct model of conduction, both terms must be due to the same conduction mechanism, implying that there is a limit to our ability to remove Fe^{3+} by lowering f_{O_2} . This limit appears to vary between olivines. The lherzolite, San Carlos olivine and San Quintin dunite have higher σ_0 terms than the Carolinian dunites and the Red Sea Peridot. The higher- σ_0 olivines are all of igneous origin and the lower- σ_0 olivines are all metamorphic; a similar correlation has been noted by *Constable et al.* [1992]. However, there is an almost perfect correlation of σ_0 with silica and iron buffering in the samples, from the lherzolite with 30% pyroxene through to the single-crystal Red Sea Peridot with no buffering at all. A similar result by *Wanamaker and Duba* [1993] on pyroxene-buffered and un-buffered San Carlos olivine lends support to the idea that the threshold conductivity is related to buffering. We show later that the time-constant for σ reequilibration after changes in f_{O_2} is almost exactly the same as for the diffusion of magnesium vacancies. Together, these observations suggest that at low f_{O_2} , V_{Mg}'' in equation (8) is being independently buffered by pyroxene and oxides,

which in turn disrupts the ability to control the population of polarons ($8Fe_{Mg}^*$) by changing f_{O_2} .

CONDUCTIVITY VERSUS TEMPERATURE

As noted above, the Mount Porndon lherzolite has more than 30% pyroxene and about 1% spinel, so the activity of silica and magnesia are buffered with possible buffering of the activity of iron, depending on the composition of the spinel. Thus, these data are likely to be representative of the conductivity of olivine with buffering of activity of all components, and a comparison with data for olivine in which activities of oxides and silica are buffered and unbuffered is likely to be instructive. For this reason, Figure 9 compares the conductivity of this lherzolite with data from *Tyburczy and Roberts* [1990] for sintered San Carlos olivine, *Roberts and Tyburczy* [1991] for San Quintin dunite, *Constable and Duba* [1990] for dunite from North Carolina, and *Schock et al.* [1989] for unbuffered San Carlos olivine. The details of the plot are informative and could be the subject of extended discourse. For example, the fayalite content of Mount Porndon olivine is about 9% and it is slightly more conductive than olivine single crystals and polycrystalline rocks with slightly higher fayalite content. This could result from the presence of the readily accessible silica buffer for the olivine grains since the sample is more than 30% pyroxene. It should also be noted that, although this effect of a pyroxene buffer on the conductivity of olivine is approximately the same as that inferred by *Wanamaker and Duba* [1993] for single crystal San Carlos olivine dusted with a coating of pyroxene, the conductivity of Mount Porndon is still slightly higher than that of the higher fayalite content San Carlos olivine. However, the principal message to be derived from a study of Figure 9 is that control of oxygen fugacity is the most important aspect of these experiments, and buffering of other activities produces only minor variations in σ at best.

DIFFUSIVITY OF f_{O_2} -INDUCED σ CHANGES

Oxygen fugacity (f_{O_2}) is changed many times throughout the experiment in steps of 1 to 4 orders of magnitude by changing the ratio of gas mix. After such a change in f_{O_2} it takes some time for σ to re-equilibrate, presumably as the effect of increased oxygen partial pressure diffuses through the sample. During the data analysis it became apparent that an attempt could be made to make a quantitative interpretation of this reequilibration process in order to extract time constants and hence diffusivity. The limitation on this analysis is that no particular effort was made during the experiment to make changes in f_{O_2} the clean step functions desirable for equilibration analysis. Thus the uncertainty in the time constants presented below is much greater than for experiments designed with this analysis in mind.

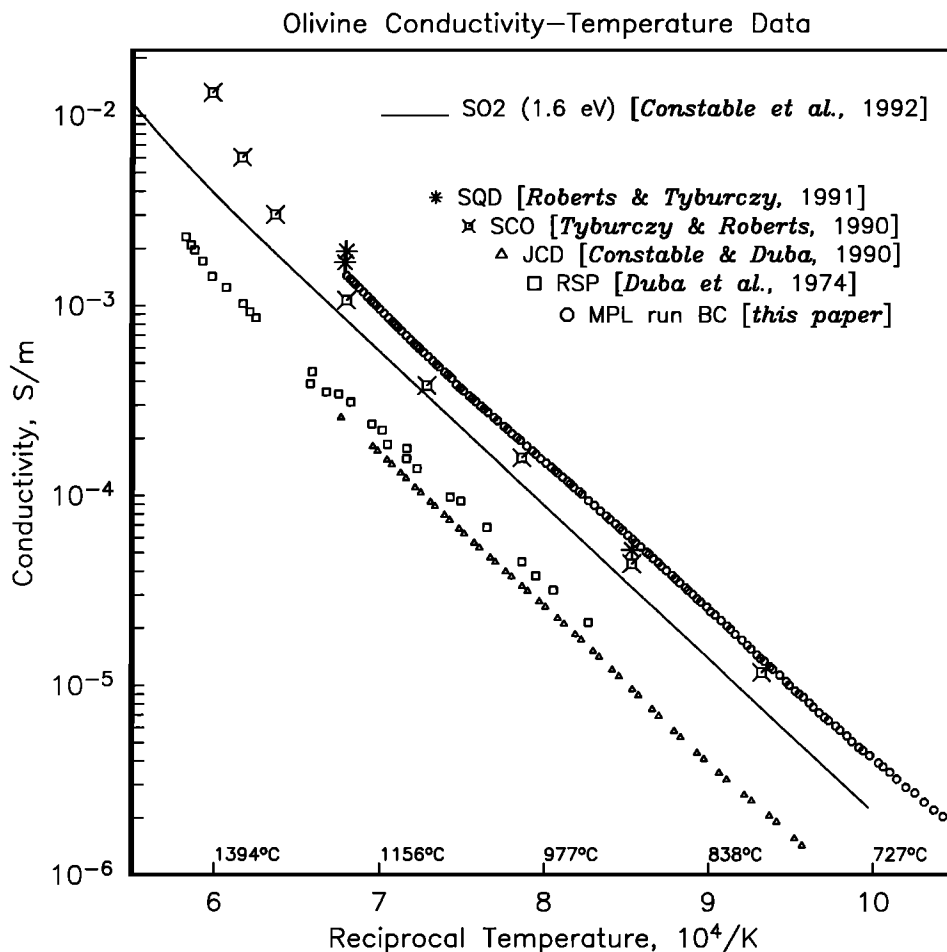


Fig. 9. Log conductivity versus reciprocal temperature for lherzolite and other olivine-dominated systems measured at or close to 10^{-3} Pa (at 1200°C). SQD, San Quintin dunite; SCO, San Carlos olivine; JCD, Jackson County dunite; RSP, Red Sea Peridot; MPL, Mount Porndon lherzolite. All samples follow an activation energy close to 1.6 eV. The main factor governing total conductivity (vertical position of the data) appears to be a grouping of metamorphic olivines (RSP and JCD) at a lower conductivity than igneous (mantle) olivines (SCO, SQD, and MPL), noted by Constable et al. [1992].

Although the sample was a circular prism, or disk, it is assumed that the experimental atmosphere can permeate the intergranular spaces of the lherzolite much more rapidly than it can diffuse into the grains. Thus, we consider the mathematics of diffusion into a sphere given a step response in external conditions. The total population of charge carriers at time t after a change in f_{O_2} is

$$n(t) = n_o \frac{4\pi a^3}{3} - n_o \frac{8a^3}{\pi} \sum_{i=1}^{\infty} \frac{e^{-i^2 \pi^2 \kappa t / a^2}}{i^2} \quad (12)$$

[Carslaw and Jaeger, 1959, p. 234; Crank, 1975, p. 91], where κ is diffusivity, a is the grain radius, and n_o is the equilibrium concentration of carriers. If we define a time constant $\tau = a^2 / \kappa$, and note that electrical conductivity is given by

$$\sigma = q\mu \frac{3}{4\pi a^3} n \quad (13)$$

where q is the charge and μ is mobility of the charge carriers, then

$$\sigma(t) = \sigma_i + \sigma_o \left[1 - \frac{6}{\pi^2} \sum_{i=1}^{\infty} \frac{1}{i^2} e^{-i^2 \pi^2 (t-t_o) / \tau} \right], \quad t \geq t_o \quad (14)$$

(we have defined t_o as the time the f_{O_2} change is made and σ_i as the initial conductivity before the change in f_{O_2}). This is a nonlinear equation, but amenable to Marquardt inversion [Marquardt, 1963], a nonlinear least squares parameter estimation procedure used successfully by, for example, Constable and Duba [1990] to estimate thermal activation energies for multiple conduction mechanisms in olivine. To apply Marquardt's method to solve for τ , σ_o , and t_o we need

$$\frac{\partial \sigma}{\partial \tau} = -\sigma_o \frac{6(t-t_o)}{\tau^2} \sum_{i=1}^{\infty} e^{-i^2 \pi^2 (t-t_o) / \tau} \quad (15)$$

$$\frac{\partial \sigma}{\partial \sigma_o} = 1 - \frac{6}{\pi^2} \sum_{i=1}^{\infty} \frac{1}{i^2} e^{-i^2 \pi^2 (t-t_o) / \tau} \quad (16)$$

$$\frac{\partial \sigma}{\partial t_o} = -\sigma_o \frac{6}{\tau} \sum_{i=1}^{\infty} e^{-i^2 \pi^2 (t-t_o) / \tau} \quad (17)$$

In practice, it requires about 4 terms of the infinite sum to obtain 1% accuracy in equation (14) at short times, but about 5 terms to obtain similar accuracy in the derivatives (equations (15), (16), and (17)). We use 40 terms in the analysis that follows.

An example of fitting equation (14) to σ reequilibration data is shown in Figure 10. Not all fits were as good, mainly as a result of failure to change the gas mix in a true step function, but also as a result of the long-term drifts in σ discussed above. To compute κ from τ we take a to be half the thickness of the sample (0.58 mm), as the sample thickness represents an upper limit on the diameter of the smallest axis of the grains, and 1 mm is a reasonable estimate of the average grain size in this rock.

Table 3 presents the results from the nonlinear fits. Standard covariance analysis as well as singular value decomposition eigenanalysis indicate very little correlation between the three fitting parameters (τ , σ_0 , and t_0). Standard errors for κ based on fitting uncertainty (statistical errors) are also given in the table. Constable *et al.* [1992] discuss some of the limitations and dangers of using these error estimates. It is clear that variations associated with systematic errors are much larger than these estimation errors in every case except BB-BC, which has an absurdly large statistical error. We believe that the systematic variations are almost entirely a result of our failure to anticipate this sort of analysis during the execution of the experiment, and that experiments in which gas mix changes were true step functions would reduce systematic errors to the level of statistical error.

In spite of the scatter in the data, the large number of measurements allow us to compute means and errors in the means at the two temperatures under consideration, and these are also given in Table 3. These means are computed on the assumption that all the data are of equal quality. We consider this to be a much more robust assumption than the idea that the fitting uncertainties reflect systematic errors arising from slow gas-mix changes and background drifts in σ . The diffusivities thus obtained and their activation energy are comparable to those obtained by Mackwell *et al.* [1988] (Figure 11) and have smaller statistical errors. Since Mackwell *et al.* interpret their diffusion data in terms of magnesium vacancies, and Schock *et*

al. [1989] interpret electrical conductivity as a consequence of polaron hopping, we must seek a logical connection between the apparent diffusivity of these two defects. The effect of f_{O_2} on σ has been addressed above and is described by equation (8):

$$8Fe_{Mg}^x + 2O_2 \rightleftharpoons 2V_{Mg}'' + V_{Si}''' + 4O_O^x + 8Fe_{Mg}^*$$

Physical and chemical properties of olivine which are dependent on f_{O_2} equilibrate on time scales much faster than oxygen can diffuse into the lattice, and so initially oxygen must be adsorbed onto, rather than absorbed into, olivine crystals and changes in oxidation state communicated to the interior by some other defect such as electrons [Boland and Duba, 1985] or metal ion vacancies [Pasteris and Wanamaker, 1988]. Polarons associated with electrical conductivity are presumably mobile compared with ionic defects [Hirsch and Shankland, 1993] and rapidly removed from the site of oxygen adsorption, and the match between σ equilibration and magnesium vacancy diffusion suggests that removal of magnesium vacancies is the rate-limiting step for adsorption of oxygen. Since diffusion of silicon is also much slower than magnesium, generation of silicon vacancies must not impede further oxygen adsorption. Alternatively, Mackwell *et al.* suggested that silicon can equilibrate internally by exchange of trivalent iron between the silicon and magnesium sites.

We discussed disequilibrium during temperature cycling earlier in the paper and showed that lack of hysteresis implied equilibrium of σ with temperature even below 900°C. Although only two points, our new data span more reciprocal temperature space than the creep data, and so an activation energy of 1.6 eV derived from them is not altogether unreliable. This is a little lower than the 1.9 eV obtained by Mackwell *et al.* [1988], and although both values lie within their uncertainties, their determination was leveraged by a low data point at 1200°C. This leverage may be eliminated by inclusion of the lower-temperature electrical data. A weighted linear regression of all the data, both creep and conductivity and using errors as given, yields an activation energy of 1.7 ± 0.3 eV. This activation energy of the f_{O_2} reequilibration process gives a time constant of 100 hours at 800°C and 5000 hours at 600°C, so it is clear that we do not have f_{O_2} equilibrium much below 900°C. That we do not see any hysteresis in σ during temperature cycling suggests that the f_{O_2} dependence of σ at these lower temperatures is very small. That is, our definite lack of f_{O_2} equilibration is not manifest as an observable effect on σ . This is consistent with the zero slope of $\sigma(f_{O_2})$ at low f_{O_2} observed for pyroxene-buffered samples at 1200°C, because below 900°C the gas mixture produces f_{O_2} s below 10^{-10} Pa, where the constant term in the f_{O_2} model (σ_0 in equation 10) dominates. There is support for this idea from the data of Wanamaker and Duba [1993] and Roberts and Tyburczy [1993], who measured $\sigma(f_{O_2})$ down to 1100 and 1000°C respectively. Examination of their data shows that at the lower temperatures the stability field of olivine does indeed migrate towards the flat part of the $\sigma(f_{O_2})$ curve. (This need not be the case, as the shape of the curve in some minerals migrates with the stability field.)

The excellent agreement with diffusivities obtained by strain measurements demonstrates the potential for the use of electrical conductivity in estimating diffusivity. Such experiments can be performed at lower temperatures (down to about 800°C) and are likely to be more precise, if not more accurate, than other methods. Even the poor quality data presented here, after

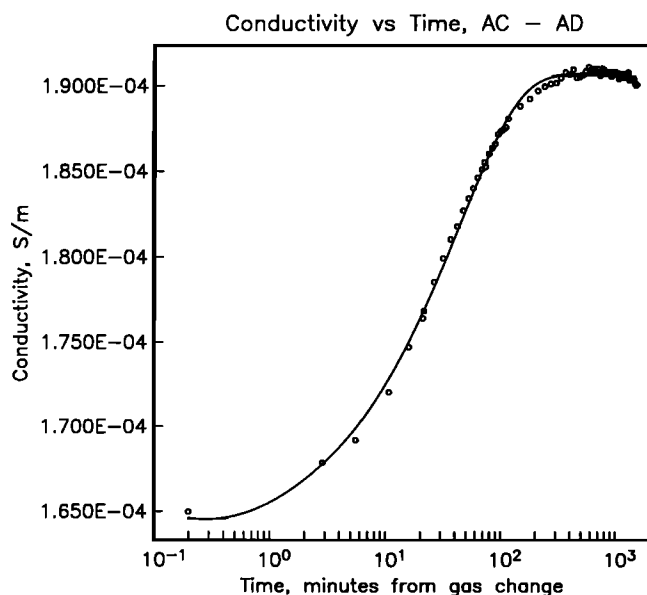


Fig. 10. Re-equilibration of run AD, immediately after a change in f_{O_2} from 10^{-4} to 10^{-2} Pa, at 1010°C. Data have been corrected for small variations in temperature around 1010°C using the known activation energy for conductivity. Several other re-equilibrations are fit as well as this one, but many are not, either as a result of drift in conductivity or failure to change the gas mix as a clean step in f_{O_2} .

TABLE 3. Fits to f_{O_2} Reequilibration Data.

Run	Temperature, C	κ , 10^{-12} m ² /s	σ_{κ}	Starting f_{O_2}	f_{O_2} Increment
AB-AC	1010	26.9	2.04	-3	-1
AC-AD	1010	10.8	0.13	-4	+2
AD-AH	1010	4.45	0.15	-2	+1
AH-AL	1010	2.07	0.07	-1	+1
AK-AL	1010	3.82	0.03	0	-4
AM-AM	1010	16.7	3.22	-4	-2
AM-AN	1010	8.28	0.25	-6	+2
AO-AP	1010	14.2	1.12	-4	+1
Simple mean	1010	10.9±2.92			
AT-AU	1200	76.9	6.09	-3	+1
AU-AV	1200	13.5	0.65	-2	+1
AV-AW	1200	14.7	0.56	-1	+1
AW-AX	1200	98.6	6.00	0	-3
AX-AY	1200	18.5	3.79	-3	-0.5
AY-AZ	1200	69.4	10.44	-3.5	-0.5
AZ-BA	1200	55.3	5.53	-4	-0.5
BA-BB	1200	79.5	3.04	-4.5	+1.5
BB-BC	1200	181	4310	-3	-2.5
BC-BC	1200	93.6	2.78	-5.5	+2.5
Simple mean	1200	70.0±15.9			

f_{O_2} values are expressed as $\log_{10}(\text{Pa})$ measured at 1200°C. σ_{κ} are one standard deviation uncertainties in κ based on the statistics of the least-squares fitting. As explained in the text, these uncertainties are not considered reliable, but do provide a relative measure of the quality of fit.

averaging, produce error bars much smaller than the variations evident in the creep studies. As an example of what might be investigated in future experiments, there is the suggestion that decreases in f_{O_2} equilibrate faster than increases in f_{O_2} . By multiplying data collected at 1010°C by the ratio of the two means, $70.3/10.9 = 6.42$, we can pool the 1010°C data with 1200°C data to provide 8 cases of decreasing f_{O_2} and 10 cases of increasing f_{O_2} . The means and error in the means thus obtained are $\kappa = 90.9 \pm 21.8 \times 10^{-12} \text{m}^2/\text{s}$ for decreasing f_{O_2} and $53.4 \pm 10.5 \times 10^{-12} \text{m}^2/\text{s}$ for increasing f_{O_2} . While this

difference is barely statistically significant, it is consistent with other, more qualitative, observations made during other studies of olivine single crystal conductivity (A. Duba and B.J. Wanamaker, unpublished data, 1993). An implication of these observations is that some kind of surface reaction plays a role in the re-equilibration process.

CONCLUSIONS

The results obtained in this study of the electrical conductivity of a mantle-derived, olivine-rich xenolith from Mount Porndon, Australia are consistent with those reported for both single-crystal and polycrystalline olivine aggregates from other localities. Such good agreement increases our confidence that laboratory measurements of olivine electrical conductivity are not liable to see any dramatic changes due to some uncontrolled parameter. Thus, we can hope to make real contributions to the interpretation of conductivity obtained by electromagnetic induction studies of Earth. The problem that occurs in making this interpretive link however, is that grain boundary phases such as carbon, oxides, fluids and melts must be considered. Geological, geochemical and other geophysical insights will be of great value in this instance. The other outstanding problem is in the transfer function used to derive the conductivity depth profile from the induction data. Contamination of the data with intervening shallow zones of high conductivity, lateral heterogeneity in crustal and mantle layers, and the trade-offs inherent in the inverse problem all contribute to a situation where the conductivity of a particular mantle region is poorly constrained.

The lherzolite is about 0.2 order of magnitude more conductive than one would expect from olivine of similar iron content. In every other respect, such as activation energy, conductivity dependence on f_{O_2} , and diffusion of the rate-limiting defect species, the rock behaves exactly the same as single crystal olivine, and so the pyroxene and spinel in the rock are not contributing directly to conductivity. However, we have interpreted drift on time scales of 50 to 100 hours as being a result of iron exchange with the pyroxene and perhaps other com-

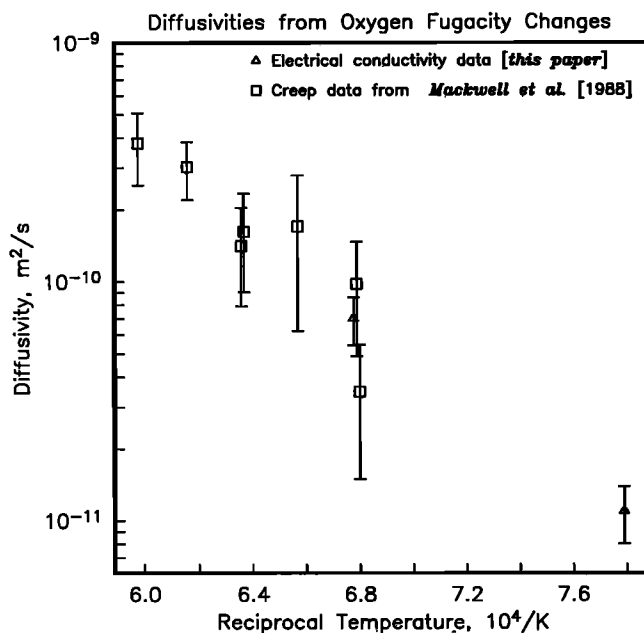


Figure 11. Diffusivity of re-equilibration in electrical conductivity after changes in f_{O_2} , as a function of reciprocal temperature. For comparison, data derived from strain rate re-equilibration by Mackwell *et al.* [1988] are also shown. Duplicate measurements collected at 1200 and 1300°C have been moved slightly in temperature for clarity of plotting error bars.

ponents of the rock, and so it is possible that we change the iron content of the olivine during the experiment. This, and the idea that this conductivity drift can provide an indication of the mantle f_{O_2} state when the rock last equilibrated, will be investigated in future studies. In order to obtain microprobe confirmation of the iron-exchange hypothesis, we shall have to either modify the apparatus to allow quenching of a sample from high temperature or perform separate 'cook and look' experiments.

Because of the higher lherzolite conductivity, it is possible that the mantle conductivity model presented by Constable *et al.* [1992], SO₂, should be revised upward slightly. On the other hand, we have seen evidence of grain-boundary resistance in series with grain interior conduction, as illustrated by Roberts and Tyburczy [1991]. A perusal of their work shows that, across the temperature range of interest, grain boundary resistance is very similar in magnitude to grain interior resistance, and so the effect is to halve the conductivity at low frequencies (below about 10–100 Hz). It is at these low frequencies that most geomagnetic estimates of mantle conductivity are made (the exception is the seafloor controlled source experiment of Cox *et al.* [1986], which operates around 8 Hz), and so one must consider lowering the lherzolite conductivities about 0.3 order of magnitude before direct application to geomagnetic soundings. However, while the pressure effect on olivine grain interior conductivity is expected to be small [Duba *et al.*, 1974], we have no idea of the pressure effect on grain boundary conduction as measured by Roberts and Tyburczy [1991]. It is not clear whether the grain boundaries of our samples are even in contact. Conventional wisdom suggests that thermal stresses will part the grain boundaries of these mm grain-size rocks on heating at atmospheric pressure, as in our experiments. That our samples generally produce reproducible results on thermal cycling and are recovered from the apparatus mostly intact suggests that this is not exactly the case. As we have noted, the sample is extremely friable at room temperature, and perhaps the grain faces are in contact at mantle temperatures, the equilibrium state for this rock. In that case they will be thermally stressed at room temperature, and perhaps our re-heating puts them in better contact than before. The effect of open microcracks on the electrical behaviour of polycrystalline rocks is a serious concern and has not been adequately addressed by any investigators experimenting on these materials. The only way to be sure that microcracks are not significantly affecting the measurements is to compare atmospheric pressure data with those from experiments under confining pressure. Unfortunately, controlling f_{O_2} under confining pressure is a technically difficult problem. In any event, SO₂ is within 0.15 order of magnitude of the conductivity of the lherzolite both before and after correction for grain boundary conduction, which is as close as one can hope to model mantle conductivity.

Acknowledgments. We would like to thank Martyn Drury for providing the rock and its compositional information and B.J. Wanamaker and Jeff Roberts for providing copies of published data. Many discussions with Lee Hirsch, Tom Shankland, and B.J. Wanamaker have undoubtedly influenced and benefited our work, and they, along with an anonymous reviewer, also gave detailed and helpful comments on the manuscript. Figures in this paper were produced using PLOTXY, courtesy of Bob Parker, who is also thanked for advice on the mathematics of diffusion. The data were collected under the support of IGPP-LLNL grant 91-47. A. Duba acknowledges the support of the Geosciences Research Program of the Office of Basic Energy Sciences. His part of the work was performed under the auspices of the

US Department of Energy at the Lawrence Livermore National Laboratory under contract W-7405-Eng-48. Work by S. Constable was conducted under support of the NSF through grants EAR-8903222 and OCE-9101783.

REFERENCES

- Boland, J.N., and A.G. Duba, An electron microscope study of the stability field and degree of nonstoichiometry in olivine, *J. Geophys. Res.*, **91**, 4711–4722, 1986.
- Buening, D.K., and P.R. Buseck, Fe-Mg lattice diffusion in olivine, *J. Geophys. Res.*, **78**, 6852–6862, 1973.
- Carlslaw, H.S., and J.C. Jaeger, *Conduction of Heat in Solids*, Oxford University Press, New York, 1959.
- Constable, S.C., and A. Duba, Electrical conductivity of olivine, a dunite and the mantle, *J. Geophys. Res.*, **95**, 6967–6978, 1990.
- Constable, S.C., T.J. Shankland, and A. Duba, The electrical conductivity of an isotropic olivine mantle, *J. Geophys. Res.*, **97**, 3397–3402, 1992.
- Cox, C.S., S.C. Constable, A.D. Chave, and S.C. Webb, Controlled source electromagnetic sounding of the oceanic lithosphere, *Nature*, **320**, 52–54, 1986.
- Crank, J., *The Mathematics of Diffusion*, Oxford University Press, New York, 1975.
- Deines, P., R.H. Nafziger, G.C. Ulmer, and E. Woermann, Temperature-oxygen fugacity tables for selected gas mixtures in the system C-H-O at one atmosphere total pressure, *Bulletin, Earth and Miner. Sci. Exp. Stn.*, Pa. State University, University Park, 1974.
- Duba, A., Electrical conductivity of Colorado oil shale to 900 C, *Fuel*, **62**, 966–972, 1983.
- Duba, A., and I.A. Nicholls, The influence of the oxidation state on the electrical conductivity of olivine, *Earth Planet. Sci. Lett.*, **18**, 59–64, 1973.
- Duba, A., J.N. Boland, and A.E. Ringwood, Electrical conductivity of pyroxene, *J. Geol.*, **81**, 727–735, 1973.
- Duba, A., H.C. Heard, and R.N. Schock, Electrical conductivity of olivine at high pressure and under controlled oxygen fugacity, *J. Geophys. Res.*, **79**, 1667–1673, 1974.
- Duba, A.G., R.N. Schock, E. Arnold, and T.J. Shankland, An apparatus for measurement of electrical conductivity to 1500°C at known oxygen fugacity, in *The Brittle-Ductile Transitions in Rocks, The Heard Volume, Geophys. Monogr. Ser.*, vol. 56, edited by A.G. Duba, W.B. Durham, J.W. Handin and H.F. Wang, pp. 207–210, AGU, Washington, D.C., 1990.
- Heinson, G. and S. Constable, The electrical conductivity of oceanic upper mantle, *Geophys. J. Int.*, **110**, 159–179, 1992.
- Hinze, E., G. Will, L. Cemič, and M. Manko, Electrical conductivity measurements on synthetic olivines at high pressures and temperatures under defined thermodynamic conditions, in *High-Pressure Researches in Geoscience*, edited by W. Schreyer, pp. 393–406, E. Schweizerbart'sche, Stuttgart, 1982.
- Hirsch, L.M., and T.J. Shankland, Quantitative olivine defect chemical model: insights on electrical conduction, diffusion, and the role of Fe impurities, *Geophys. J. Int.*, in press, 1993.
- Hirsch, L.M., T.J. Shankland, and A.G. Duba, Electrical conductivity and mobility in olivine (abstract), *Eos Trans. AGU*, **70**, 1369, 1989.
- Huebner, J.S., A. Duba, and L.B. Wiggins, Electrical conductivity of pyroxene which contains trivalent cations: laboratory measurements and the lunar temperature profile, *J. Geophys. Res.*, **84**, 4652–4656, 1979.
- Irving, A.J., Petrology and geochemistry of composite ultramafic xenoliths in alkalic basalts and implications for magmatic processes in the mantle, *Am. J. Sci.*, **280**, 389–426, 1980.
- Kariya, K.A., and T.J. Shankland, Electrical conductivity of dry lower crustal rocks, *Geophysics*, **48**, 52–61, 1983.
- Mackwell, S.J., D. Dimos, and D.L. Kohlstedt, Transient creep of olivine: Point-defect relaxation times, *Philos. Mag. A*, **57**, 779–789, 1988.
- Marquardt, D.W., An algorithm for least-squares estimation of non-linear parameters, *J. Soc. Ind. Appl. Math.*, **11**, 431–441, 1963.
- Olhoeft, G.R., Electrical properties of granite with implications for the lower crust, *J. Geophys. Res.*, **86**, 931–936, 1981.
- Parkhomenko, E.I., *Electrical Properties of Rocks*, Plenum, New York, 1967.
- Pasteris, J.D., and B.J. Wanamaker, Laser Raman microprobe analysis of experimentally re-equilibrated fluid inclusions in olivine: Some

- implications for mantle fluids, *Am. Mineral*, *73*, 1074–1088, 1988.
- Rai, C.S., and M.H. Manghnani, Electrical conductivity of basic and ultrabasic rocks as a function of temperature to 1500°C, *Phys. Earth Planet. Inter.*, *17*, 6–13, 1978.
- Roberts, J.J., and J.A. Tyburczy, Frequency dependent electrical properties of polycrystalline olivine compacts, *J. Geophys. Res.*, *96*, 16, 205–16,222, 1991.
- Roberts, J.J., and J.A. Tyburczy, Frequency dependent electrical properties of dunite as functions of temperature and oxygen fugacity, *Phys. Chem. Miner.*, in press, 1993.
- Sato, H., High temperature a.c. electrical properties of olivine single crystal with varying oxygen partial pressure: Implications for the point defect chemistry, *Phys. Earth Planet. Inter.*, *41*, 269–282, 1986.
- Shankland, T.J., A.G. Duba, B.J. Wanamaker, and L.M. Hirsch, Attaining thermodynamic equilibrium in electrical conductivity measurements of minerals (abstract), *Eos, Trans. AGU*, *72*, (44) Fall Meeting suppl., 123, 1991.
- Schock, R.N., A. Duba, and T.J. Shankland, Electrical conduction in olivine, *J. Geophys. Res.*, *94*, 5829–5839, 1989.
- Tyburczy, J.A., and J.J. Roberts, Low frequency electrical response of polycrystalline olivine compacts: Grain boundary transport, *Geophys. Res. Lett.*, *17*, 1985–1988, 1990.
- Wanamaker, B.J., and A.G. Duba, Electrical conductivity of San Carlos olivine along [100] under oxygen- and pyroxene-buffered conditions and implications for defect equilibria, *J. Geophys. Res.*, *98*, 489–500, 1993.
-
- S. Constable, Scripps Institution of Oceanography, La Jolla, CA 92093-0225.
- A. Duba, Lawrence Livermore National Laboratory, L201, Livermore, CA 94550.

(Received July 30, 1992;
revised February 1, 1993;
accepted April 12, 1993.)